


Eccentric pie charts and an unusual pie cutting

Sándor Bozóki 

Information Visualization
2020, Vol. 19(4) 288–295
© The Author(s) 2020
Article reuse guidelines:
sagepub.com/journals-permissions
DOI: 10.1177/1473871620925078
journals.sagepub.com/home/ivi


Abstract

The eccentric pie chart, a generalization of the traditional pie chart is introduced. An arbitrary point is fixed within the circle, and rays are drawn from it. A sector is bounded by a pair of neighboring rays and the arc between them. Eccentric pie charts have the potential of visualizing multiple sets of data, especially for small numbers of items/features. The calculations of the area-proportional diagram are based on well-known equations in coordinate geometry. The resulting system of polynomial and trigonometric equations can be approximated by a fully polynomial system, once the non-polynomial functions are approximated by their Taylor series written up to the first few terms. The roots of the polynomial system have been found by the homotopy continuation method, then used as starting points of a Newton iteration for the original (non-polynomial) system. The method is illustrated on a special pie-cutting problem.

Keywords

Eccentric pie chart, area-proportional diagram, pie cutting, multivariate polynomial system, homotopy continuation method

Introduction

Pie chart is more than 200 years old. According to Spence¹ and Tufte² [p. 44], Playfair³ [Chart 2 on p. 49] invented it. The popularity of the traditional pie chart is rooted in its simplicity and efficiency in visualization. For an arbitrary set of $n \geq 2$ positive numbers $\lambda_i, i = 1, \dots, n$ such that $\lambda_1 + \lambda_2 + \dots + \lambda_n = 1$, the corresponding circle sectors in the pie chart visualize the relative magnitude of numbers λ_i in three equivalent ways: (a) areas, (b) central angles, (c) arc lengths are proportional to the numbers λ_i . Kosara⁴ surveys the perceptual studies and provides experimental results on projected pie charts.

Area proportionality can be important in data visualization, for example, in case of Venn diagrams, where the sizes of the sets (represented by circles) as well as the overlaps correspond to the cardinalities in the data sets from biological lists.⁵

The *pizza theorem*^{6–8} states that the $2n$ -blade ($n \geq 2$ is even) equiangular cutter, wherever it is located, halves the circle's area by summing the areas of the alternate eccentric sectors, see Figure 1.

If the traditional pie chart is modified such that the center, the common point of the sectors is moved from the circle's center, an eccentric pie chart is resulted. Consider a point inside the unit circle and draw rays from it. A sector is bounded by a pair of neighboring rays and the arc between them (Figure 2). We focus on the area of the sectors. Unlike in case of the traditional pie chart, the angle of the neighboring rays and the arc length are not proportional to the sector's area any more.

The goals of the article are to apply the idea of eccentric pie chart, a special type of area proportional diagrams, such as the left parts of Figures 3 and 4 (explained and detailed by the middle and right parts) and Figure 5, to visualize single or multiple sets of data; and to present some mathematical details of the calculations.

Institute for Computer Science and Control (SZTAKI), Corvinus University of Budapest, Budapest, Hungary

Corresponding author:

Sándor Bozóki, SZTAKI, Kende str. 13-17, 1111 Budapest, Hungary.
Email: bozoki.sandor@sztaki.hu

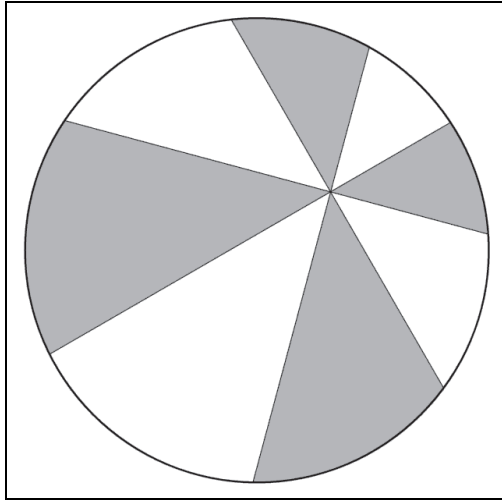


Figure 1. The total area of gray sectors is equal to the total area of white sectors (pizza theorem for $n=4$).

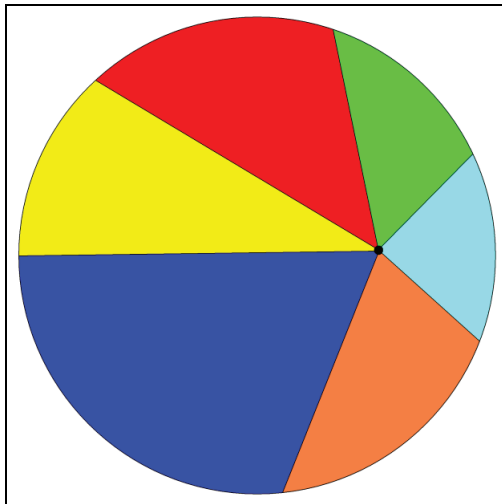


Figure 2. An eccentric pie chart.

Figure 3 presents a simple situation, where, for example, 70% of the effects (large circle) come from 25% of the causes (small circle), similar to the Pareto 80/20 principle but with different numbers. Here, the size of the small circle is irrelevant, it does not have a specific meaning, therefore its boundary is not drawn.

Figure 4 presents the ratio of Internet users in the world, Europe and Russia based on the data in Table 1. The diagram is completely area proportional: the areas of the circles are proportional to the populations and the areas of the sectors are proportional to the numbers of people using or not using Internet, worldwide, in Europe and in Russia.

Figure 5 compares the age structures of world's population in 1968 (small circle) and 2018 (large

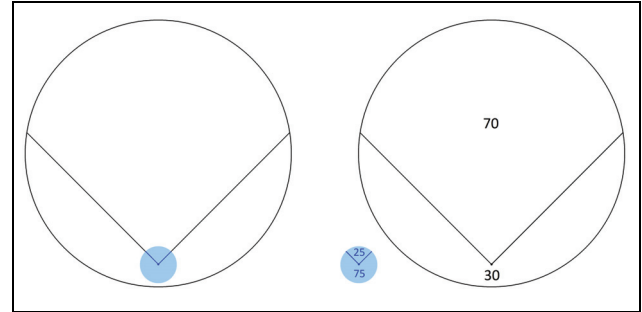


Figure 3. An area proportional eccentric pie chart visualizing the situation 70% of the effects (large circle) come from 25% of the causes (small circle).

Table 1. Internet use and population statistics in 2019, population numbers rounded to millions, percentages rounded to integers (source: Internet World Stats⁹).

	Population (million)	Internet users (million)	Internet users/population (%)
World	7716	4536	59
Europe	829	727	88
Russia	144	116	81

Table 2. The age structures of the world's population in 1968 and 2018 (source: World Bank¹⁰).

Age group	Population in 1968 (million)	Population in 2018 (million)
0–14 years	1337 (37.8%)	1959 (25.8%)
15–64 years	2012 (57%)	4961 (65.3%)
65 + years	184 (5.2%)	674 (8.9%)
Total	3533	7594

circle), based on the World Bank's data¹⁰ in Table 2. The circles' areas are proportional to the total populations, so are the sectors to the age groups.

The sketch of the calculations is as follows. The eccentric sector's area is derived from the areas of a circular sector and two triangles. The geometrical problem is transformed to an algebraic one by formulas of coordinate geometry, resulting in a system of nonlinear, namely polynomial and trigonometric, equations. Systems of nonlinear equations are usually hard to solve [Chapter 11¹¹]. If all equations are polynomial, homotopy continuation methods^{12,13} can be applied. HOM4PS-3¹³ is used in this article. Several geometric problems, such as Littlewood's problem on seven mutually touching infinite cylinders,¹⁴ or Steiner's conic problem¹⁵ lead to polynomial

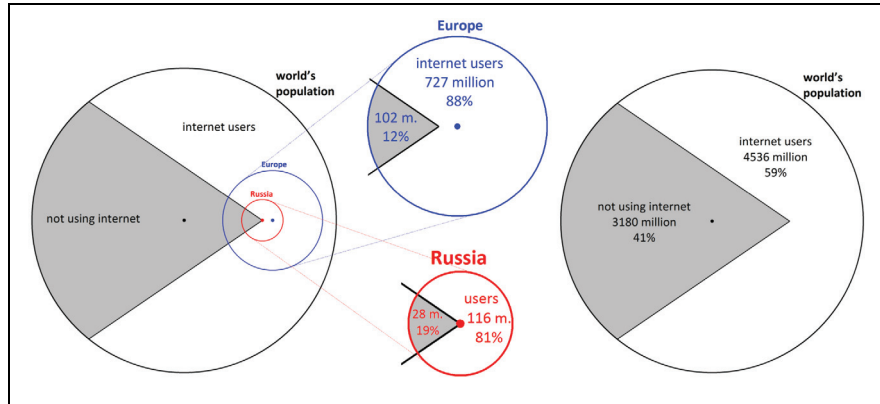


Figure 4. An area proportional eccentric pie chart visualizing the Internet penetration in the world, Europe and Russia, based on the data in Table 1.

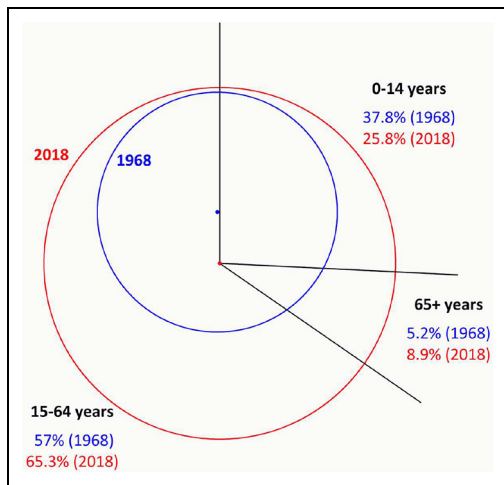


Figure 5. An area-proportional eccentric pie chart for the comparison of the age structures of world's population in 1968 and 2018, based on the data in Table 2.

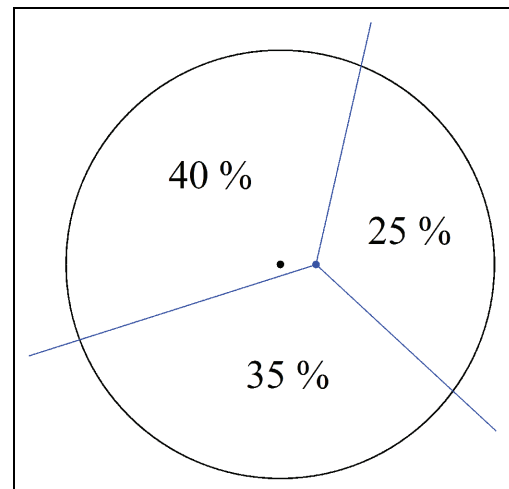


Figure 6. 40%-35%-25% pie cutting with a regular three-blade cutter.

equations. The equations of the eccentric pie chart include non-polynomial ones; however, an approximation by the Taylor series, written up to the first few terms, is polynomial. This idea of polynomial approximation has also been applied by Ji et al.¹⁶ [Example 4.4], Lim,¹⁷ and Yalçınbaş.¹⁸ The roots of the approximating polynomial system can be found by the homotopy method,¹³ then they are used as starting points of a Newton iteration for the approximated system of non-polynomial equations.

The calculation of area-proportional eccentric pie chart is illustrated through a geometrical problem. Assume that a circular pie is to be distributed among three children such that their shares are proportional to the children's time spent with assisting, 40, 35, and 25 min. There is a three-blade pie (or pizza) cutter in

the kitchen, but it is designed for equal slices: the angle of every pair of blades is 120° . Where to locate the cutter in order to get slices of area 40%, 35%, and 25% of the whole pie? The answer is shown in Figure 6.

The rest of the article is structured as follows. The eccentric pie chart is introduced in section "Eccentric pie charts," where the general steps of the calculations are presented, too. These steps are specified in section "Pie cutting with a multi-blade cutter," where the complete and detailed solution of the 40%-35%-25% pie-cutting problem above is presented. The nonlinear system has nine equations of nine variables, its polynomial approximation leads to a system of 11 polynomial equations of 11 variables. Section "Conclusion" concludes the article, and limitations and future research directions are also discussed.

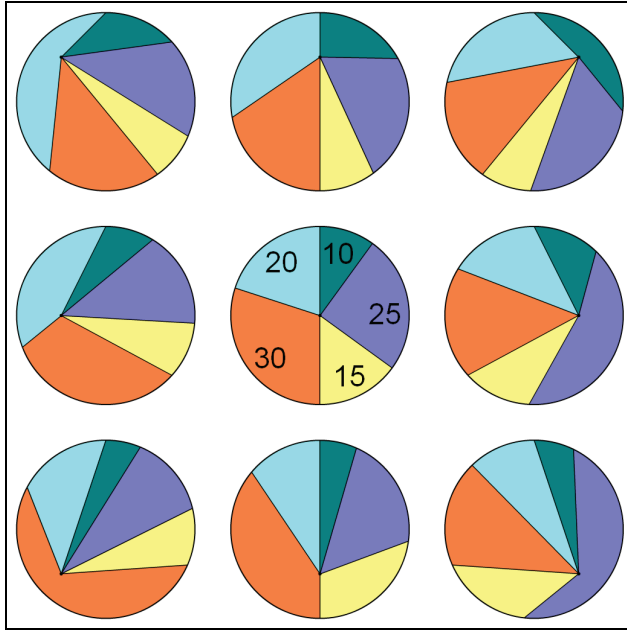


Figure 7. Eccentric pie charts with areas 20%-30%-15%-25%-10%, where $x_0, y_0 \in \{-1/2, 0, 1/2\}$.

Eccentric pie charts

Once the center is moved from the circle's center, as it was shown in Figure 2, there are infinitely many eccentric pie charts representing the same set of proportions (percentages). In fact, the degree of freedom of eccentric pie charts is 2, if rotations of the circle are not distinguished. Once the starting point, for example, $(0,1)$, on the boundary of the circle is fixed, the point (x_0, y_0) can be located anywhere inside the unit circle, there exists exactly one eccentric pie chart representing the given set of proportions counterclockwise, and another one clockwise. Figure 7 shows nine eccentric pie charts ($x_0, y_0 \in \{-1/2, 0, 1/2\}$), all of them visualize the 20%-30%-15%-25%-10% counterclockwise. The first ray is between points (x_0, y_0) and $(0,1)$. The pie chart in the middle is the traditional pie chart.

Figure 7 suggests that if there is a single level of data, the eccentric pie charts are not necessarily more convenient to “read,” compared to the traditional pie chart in the middle. However, if multiple levels of data are displayed, as shown in Figures 3–5, the eccentric pie charts seem applicable.

The areas of eccentric sectors can be calculated as follows. Figures 8 and 9 show the possible arrangements, a circular sector and two triangles are necessary and sufficient to express the eccentric sector's area. Let (x_1, y_1) and (x_2, y_2) be two points on the boundary of the unit circle centered at the origin. The area of a circular sector is equal to $\beta/2$, where β is the central

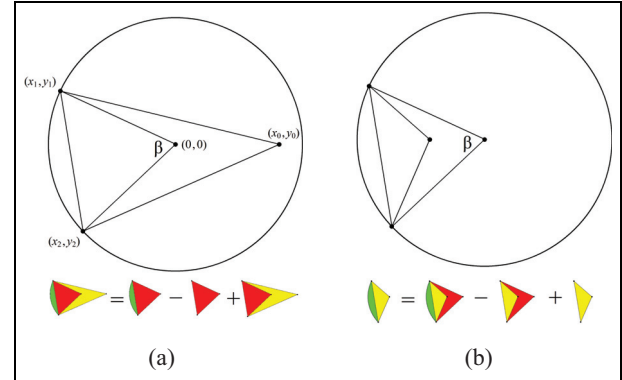


Figure 8. The calculation of the eccentric sector's area ($\beta < \pi$).

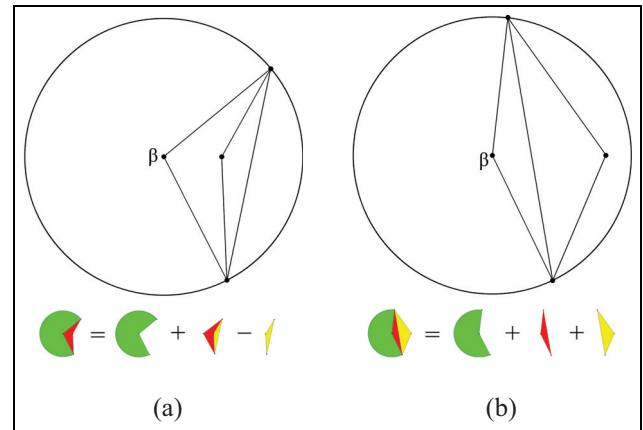


Figure 9. The calculation of the eccentric sector's area ($\beta > \pi$).

angle. It is also well known that $x_1x_2 + y_1y_2 = \cos\beta$. The area of the triangle (x_1, y_1) , (x_2, y_2) , $(0,0)$ is $\sin\beta/2$, if $\beta < \pi$ (Figure 8), and $\sin(2\pi - \beta)/2$, if $\beta > \pi$ (Figure 9).

The area of a triangle can be directly calculated from the coordinates of its vertices.

Lemma 2.1. [See, e.g. (Problem 52 on p. 34 of Fine and Thompson¹⁹) or (formula [4.7.2] on p. 212 of Zwillinger²⁰)]. The area of triangle (x_1, y_1) , (x_2, y_2) , (x_0, y_0) is equal to

$$\begin{aligned} & \frac{1}{2} \left| \det \begin{pmatrix} x_1 & y_1 & 1 \\ x_2 & y_2 & 1 \\ x_0 & y_0 & 1 \end{pmatrix} \right| \\ &= \frac{1}{2} |x_1y_2 + x_2y_0 + x_0y_1 - x_2y_1 - x_0y_2 - x_1y_0| \end{aligned} \quad (1)$$

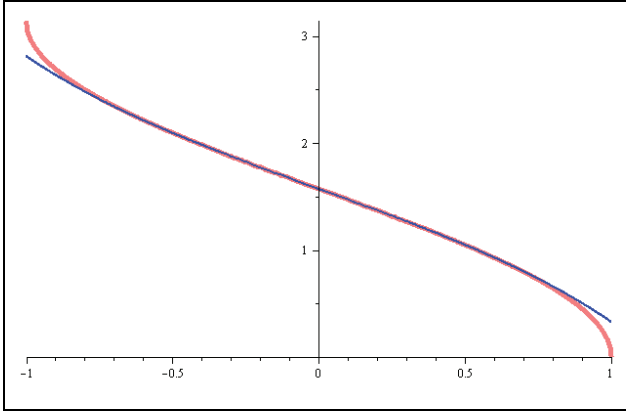


Figure 10. $\arccos(x)$ and its Taylor series around $a=0$ up to six terms.

Now, let us prescribe that the area of the eccentric sector $(x_1, y_1), (x_2, y_2), (x_0, y_0)$ with central angle $\beta < \pi$ must be $\lambda\pi$, where $\lambda < 1$ is given. The following equations can be written

$$x_1x_2 + y_1y_2 = \cos\beta \quad (2)$$

$$2\left(\lambda\pi - \frac{\beta}{2} + \frac{\sin\beta}{2}\right) \quad (3)$$

$$= |x_0(y_1 - y_2) + x_1(y_2 - y_0) + x_2(y_0 - y_1)|$$

$$x_1^2 + y_1^2 = 1 \quad (4)$$

$$x_2^2 + y_2^2 = 1 \quad (5)$$

The system of equations above includes both polynomials and trigonometric expressions, which is hard to solve. Since there exist powerful algorithms^{12,13} for solving polynomial systems, our aim is to build a polynomial system, which is *close* to the non-polynomial system (2)–(5). Replace $\sin\beta$ by the new variable s_β and consider the non-polynomial equation $\beta = \arccos(x_1x_2 + y_1y_2)$ from equation (2).

Lemma 2.2. (See, e.g. (Section 1.9.4.2 on p. 50 and Section 1.9.6.5 on p. 61 of Zwillinger²⁰))

The Taylor series of function \arccos around a is

$$\arccos(x) = \sum_{n=0}^{\infty} \frac{\arccos^{(n)}(a)}{n!} (x-a)^n \quad (6)$$

especially with $a = 0$

$$\begin{aligned} \arccos(x) &= \frac{\pi}{2} - \sum_{n=0}^{\infty} \frac{(2n)!}{4^n (n!)^2 (2n+1)} x^{2n+1} \\ &= \frac{\pi}{2} - x - \frac{1}{6}x^3 - \frac{3}{40}x^5 + O(x^7), (|x| < 1) \end{aligned} \quad (7)$$

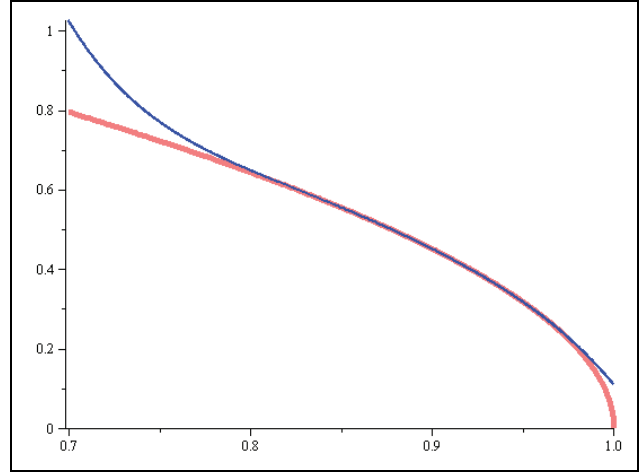


Figure 11. $\arccos(x)$ and its Taylor series around $a=0.9$ up to six terms.

Figure 10 shows that the Taylor series around $a = 0$ up to six terms approximates the \arccos function well if $|x| < 0.8$. If $|x|$ is close to 1, the Taylor series around $a = 0.9$ up to six terms provides a good approximation (Figure 11). Then one of the equations (6) and (7) with $x = x_1x_2 + y_1y_2$ results in a multivariate polynomial. The absolute values in equation (3) can be eliminated by taking the squares of both sides of the equation (false roots are possible and they have to be filtered out).

A detailed specification of the calculations is given in the next section, where the pie-cutting problem is solved.

Pie cutting with a multi-blade cutter

Let us solve the 40%-35%-25% pie-cutting problem from the end of section “Introduction” (Figure 6), by using the methods presented in section “Eccentric pie charts.” Let us have a unit circle with its center in the origin. Denote by (x_0, y_0) the coordinates of the three-blade cutter’s center. We can assume that $y_0 = 0$ due to rotational symmetry. $-1 < x_0 < 1$ is assumed in an implicit way: no equation is generated, but after the system of equations is solved, roots not satisfying this double inequality are filtered out.

Denote by (x_1, y_1) , (x_2, y_2) , and (x_3, y_3) the coordinates of the three points, where the boundary of the circle and the blades meet, as in Figure 12. Let β denote the central angle of the first eccentric sector (of area $\lambda_1\pi = 0.4\pi$) bounded by line sections $[(x_0, 0), (x_1, y_1)]$ and $[(x_0, 0), (x_2, y_2)]$ and the arc between them. Similarly, let φ denote the central angle of the second eccentric sector (of area $\lambda_2\pi = 0.35\pi$) bounded by line sections $[(x_0, 0), (x_2, y_2)]$ and

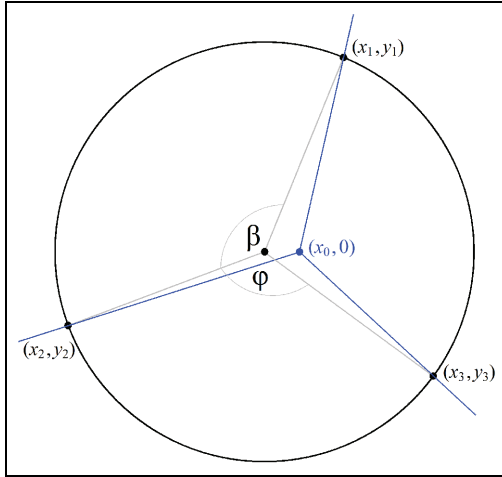


Figure 12. Pie cutting with a regular three-blade cutter.

$[(x_0, 0), (x_3, y_3)]$ and the arc between them. The third eccentric sector's area is $\lambda_3\pi = 0.25\pi$, and its central angle is $2\pi - \beta - \varphi$.

Following section "Eccentric pie charts" and including the regularity of three-blade cutter (pairwise angles are $2\pi/3$) we have the following equations

$$(x_1x_2 + y_1y_2)^2 + \sin^2\beta = 1 \quad (8)$$

$$(x_2x_3 + y_2y_3)^2 + \sin^2\varphi = 1 \quad (9)$$

$$\begin{aligned} 2\lambda_1\pi - \beta + \sin\beta \\ = |x_0(y_1 - y_2) + x_1(y_2 - y_0) + x_2(y_0 - y_1)| \end{aligned} \quad (10)$$

$$\begin{aligned} 2\lambda_2\pi - \varphi + \sin\varphi \\ = |x_0(y_2 - y_3) + x_2(y_3 - y_0) + x_3(y_0 - y_2)| \end{aligned} \quad (11)$$

$$x_1^2 + y_1^2 = 1 \quad (12)$$

$$x_2^2 + y_2^2 = 1 \quad (13)$$

$$x_3^2 + y_3^2 = 1 \quad (14)$$

$$\begin{aligned} (x_1 - x_0)(x_2 - x_0) + (y_1 - y_0)(y_2 - y_0) = \cos\left(\frac{2\pi}{3}\right) \\ \sqrt{[(x_1 - x_0)^2 + (y_1 - y_0)^2][(x_2 - x_0)^2 + (y_2 - y_0)^2]} \end{aligned} \quad (15)$$

$$\begin{aligned} (x_2 - x_0)(x_3 - x_0) + (y_2 - y_0)(y_3 - y_0) = \cos\left(\frac{2\pi}{3}\right) \\ \sqrt{[(x_2 - x_0)^2 + (y_2 - y_0)^2][(x_3 - x_0)^2 + (y_3 - y_0)^2]} \end{aligned} \quad (16)$$

where $\lambda_1 = 0.4$, $\lambda_2 = 0.35$, $y_0 = 0$ and $\cos(2\pi/3) = -1/2$.

Introduce variables s_β , s_φ to replace $\sin\beta$ and $\sin\varphi$, respectively. In order to avoid absolute values in equations (10)–(11), take the squares of both sides. This step may bring false solutions, and we will see that it

does so indeed. The square root in equations (15) and (16) can be eliminated likewise, with another possibility to have false solutions. Equations (8)–(11), (15), and (16) are replaced by polynomial equations

$$(x_1x_2 + y_1y_2)^2 + s_\beta^2 = 1 \quad (17)$$

$$(x_2x_3 + y_2y_3)^2 + s_\varphi^2 = 1 \quad (18)$$

$$\begin{aligned} (2\lambda_1\pi - \beta + s_\beta)^2 \\ = [x_0(y_1 - y_2) + x_1(y_2 - y_0) + x_2(y_0 - y_1)]^2 \end{aligned} \quad (19)$$

$$\begin{aligned} (2\lambda_2\pi - \varphi + s_\varphi)^2 \\ = [x_0(y_2 - y_3) + x_2(y_3 - y_0) + x_3(y_0 - y_2)]^2 \end{aligned} \quad (20)$$

$$\begin{aligned} [(x_1 - x_0)(x_2 - x_0) + (y_1 - y_0)(y_2 - y_0)]^2 \\ = \frac{1}{4}[(x_1 - x_0)^2 + (y_1 - y_0)^2] \end{aligned} \quad (21)$$

$$\begin{aligned} [(x_2 - x_0)(x_3 - x_0) + (y_2 - y_0)(y_3 - y_0)]^2 \\ = \frac{1}{4}[(x_2 - x_0)^2 + (y_2 - y_0)^2] \\ [(x_3 - x_0)(x_4 - x_0) + (y_3 - y_0)(y_4 - y_0)]^2 \end{aligned} \quad (22)$$

Finally approximate the equations

$$\cos\beta = x_1x_2 + y_1y_2 \quad (23)$$

$$\cos\varphi = x_2x_3 + y_2y_3 \quad (24)$$

or, equivalently, $\beta = \arccos(x_1x_2 + y_1y_2)$ and $\varphi = \arccos(x_2x_3 + y_2y_3)$ by the Taylor series of function \arccos around zero up to the fifth power as in equation (7). Here, we expect that angles β and φ are between $\arccos(0.8) \approx 0.6435 \approx 37^\circ$ and $\pi - \arccos(0.8) \approx 2.498 \approx 143^\circ$. If this assumption fails, we can try the other Taylor series around 0.9 as in equation (6) and Figure 11

$$\begin{aligned} \beta = \frac{\pi}{2} - (x_1x_2 + y_1y_2) - \frac{1}{6}(x_1x_2 + y_1y_2)^3 \\ - \frac{3}{40}(x_1x_2 + y_1y_2)^5 \end{aligned} \quad (25)$$

$$\begin{aligned} \varphi = \frac{\pi}{2} - (x_2x_3 + y_2y_3) \\ - \frac{1}{6}(x_2x_3 + y_2y_3)^3 - \frac{3}{40}(x_2x_3 + y_2y_3)^5 \end{aligned} \quad (26)$$

The system of polynomial equations (12)–(14), (17)–(22), and (25)–(26) has 11 equations and 11 variables: $x_0, x_1, y_1, x_2, y_2, x_3, y_3, \beta, \varphi, s_\beta$, and s_φ . Homotopy algorithm HOM4PS-3¹³ found 28,224 roots, 720 of them are real. However, most of them are false solutions to the geometric problem, due to several reasons. Many roots do not fulfill $|x_0|, |s_\beta|, |s_\varphi| \leq 1$. Some roots satisfy (19)/(20) but not (10)/(11), or, similarly, satisfy (21)/(22) but not (15)/(16). Furthermore, $s_\beta \neq \sin\beta$, but instead of that $s_\beta \approx -\sin\beta$.

After all four solutions remain to use as starting points of a Newton iteration for the system of equations (12)–(14) and (17)–(24). Maple's *fsolve* refines the solution with an arbitrary accuracy. However, we observed that the roots calculated from the polynomial system were already within an error of 0.002 for all variables, which is due to that the Taylor series provided a good polynomial approximation of the function.

The four solutions are essentially the same: one solution, given below up to 10 correct digits

$$\begin{aligned}x_0 &= 0.164641996 \\x_1 &= 0.375176778 \\y_1 &= 0.926953281 \\x_2 &= -0.939722783 \\y_2 &= -0.341937259 \\x_3 &= 0.805164109 \\y_3 &= -0.593052069 \\\beta &= 2.304361451 \approx 132^\circ \\\varphi &= 2.157770813 \approx 123.6^\circ \\s_\beta &= \sin \beta = 0.742792198 \\s_\varphi &= \sin \varphi = 0.832620150\end{aligned}$$

has already been shown in Figures 6 and 12, the others are its reflections on the vertical and/or horizontal axes.

The relatively small value of $x_0 \approx 0.1646$ shows the high level of sensitivity of the proportions, once the center of removed from the origin, even by a little.

Note that λ_i ($i = 1, 2, 3$) cannot be arbitrary in this problem. Even if the center (x_0, y_0) is located at $(1, 0)$, that is, on the circle's border, the largest sector's area is at most $\pi - 2((\pi/6) - (\sqrt{3}/4)) \approx 0.9423\pi$.

Conclusion

Motivated by the area-proportional comparisons of multi-level data in Figures 4–6, eccentric pie charts, their potential applications in data visualization and methods for calculations are studied in the article.

Some limitations of eccentric pie charts have already appeared in this first study and during the calculations behind. Although the geometric derivation is simple, the calculations of the areas, as witnessed in sections “Eccentric pie charts” and “Pie cutting with a multi-blade cutter,” are not elementary. The current proposal is far from the implementation of an easy-to-use software. As Figure 7 showed, the traditional pie chart seems better if single proportions are displayed. However, Figures 4–6 suggest that the comparisons of two or three objects with respect to two or three features are feasible with eccentric pie charts.

The example in Figure 5 and Table 2 suggests that if we insist on that only one circle can be eccentric, not both of them, then three is the tight upper bound for the number of categories. This observation is supported by the counting of degrees of freedom: if we depart from the small circle with its given proportions (second column in Table 2) and rays, the center of the large circle can be chosen from a two-dimensional space, exactly the same number as the degree of freedom of the possible sets of three proportions (third column in Table 2) in the large circle. Four or more age categories would already lead to an overdetermined system of equations. If both circles can be eccentric, that is, none of their centers coincides with the center of the radii, then five is the tight upper bound for the number of categories.

Constraints on proportions that can be displayed by eccentric pie charts, belong to another type of limitations. For example, the classical 80–20 Pareto principle cannot be plotted similar to Figure 3. Even if the center of the small circle is located at large circle's border, the small circle's central angle $2\pi/5$ corresponding to 20% cuts only $\approx 70.27\%$ of the large circle's area.

The method of solving non-linear, non-polynomial systems through their polynomial approximation, presented in section “Eccentric pie charts” and illustrated on an example in section “Pie cutting with a multi-blade cutter,” is applicable to larger systems, too. The replacement of a non-polynomial function by its Taylor series or other polynomial approximations, has practical limitations, because a polynomial system can also be hopelessly hard to solve.

The exact structure and dimensions of multiple data sets that can be visualized by eccentric pie charts, is not discovered yet. As the aforementioned constraints on data restrictions show that counting the degrees of freedom is only necessary but not always sufficient.

Future studies might include experimental studies of visual perception, as the ones performed with the traditional pie charts (see Kosara⁴ (subsection 2.1)) and, for example, their rotations in the space.⁴ A possible outcome of such experiments can be that visual perception generates stricter constraints compared to the mathematical bounds mentioned above.

Funding

The author(s) disclosed receipt of the following financial support for the research, authorship, and/or publication of this article: This work was supported by the Hungarian National Research, Development and Innovation Office (NKFIH) under Grant NKFIA ED_18-2-2018-0006.

ORCID iD

Sándor Bozóki  <https://orcid.org/0000-0003-4170-4613>

References

1. Spence I. No humble pie: the origins and usage of a statistical chart. *J Educ Behav Stat* 2005; 30(4): 353–368.
2. Tufte ER. *The visual display of quantitative information*. 2nd ed. Cheshire, CT: Graphics Press, 2001.
3. Playfair W. *The statistical breviary*. London: T. Bensley, 1801.
4. Kosara R. Evidence for area as the primary visual cue in pie charts. In: *Proceedings of the 2019 IEEE visualization conference (VIS)*, Vancouver, BC, Canada, 20–25 October 2019, pp. 101–105. New York: IEEE.
5. Hulsen T, de Vlieg J and Alkema W. BioVenn—a web application for the comparison and visualization of biological lists using area-proportional Venn diagrams. *BMC Genomics* 2008; 9: 488.
6. Mabry R and Deiermann P. Of cheese and crust: a proof of the pizza conjecture and other tasty results. *Am Math Mon* 2009; 116(5): 423–438.
7. Ornes S. As easy as pie. *New Sci* 2009; 204(2738): 48–50.
8. Upton LJ. Problem 660. *Math Mag* 1967; 40(3): 163.
9. Internet WorldStats. World Internet users and 2019 population stats; Internet user statistics & 2019 population for the 53 European countries and regions, 2020, <https://www.internetworldstats.com/stats4.htm>
10. World Bank. Population (total); Population by age, 2020, <https://data.worldbank.org/indicator/SP.POP.TOTL?end=2018&locations=1W&start=1960&view=chart>
11. Nocedal J and Wright SJ. *Numerical optimization*. 2nd ed. Cham: Springer, 2006.
12. Lee TL, Li TY and Tsai CH. HOM4PS-2.0: a software package for solving polynomial systems by the polyhedral homotopy continuation method. *Computing* 2008; 83: 109–133.
13. Chen T, Lee T-L and Li T-Y. Mixed cell computation in Hom4PS-3. *J Symb Comput* 2017; 79(3): 516–534.
14. Bozóki S, Lee TL and Rónyai L. Seven mutually touching infinite cylinders. *Comput Geom: Theory Appl* 2015; 48(2): 87–93.
15. Breiding P, Sturmfels B and Timme S. 3264 conics in a second. *Notices of the American Mathematical Society* 2020; 67(1): 30–37.
16. Ji Z, Wu W, Feng Y, et al. Numerical method for real root isolation of semi-algebraic system and its applications. *J Comput Theor Nanos* 2016; 13(1): 803–811.
17. Lim T-C. Application of Maclaurin series in relating interatomic potential functions: a review. *J Math Chem* 2004; 36(2): 147–160.
18. Yalçınbaş S. Taylor polynomial solutions of nonlinear Volterra-Fredholm integral equations. *Appl Math Comput* 2002; 127(2–3): 195–206.
19. Fine HB and Thompson HD. *Coordinate geometry*. New York: Macmillan, 1909.
20. Zwillinger D (ed.) *CRC standard mathematical tables and formulas*. 33rd ed. London: CRC Press, 2018.